Title

Sediment Residence Times in Large Rivers Quantified Using a Cosmogenic Nuclides Based Transport Model and Implications for Buffering of Continental Erosion Signals

Journal

Journal of Geophysical Research Earth Surface, 127(5)

ISSN

2169-9003

Authors

Ben-Israel, Michal
Armon, Moshe
Team, ASTER
et al.

Publication Date

2022-05-01

DOI

10.1029/2021jf006417

Sediment Residence Times in Large Rivers Quantified Using a Cosmogenic Nuclides Based Transport Model and Implications for Buffering of Continental Erosion Signals

Michal Ben-Israel[1,2], Moshe Armon[1,3], ASTER Team[4]†, and Ari Matmon[1]

[1]The Institute of Earth Sciences, Hebrew University of Jerusalem, Jerusalem, Israel.

[2]Department of Life and Environmental Sciences, University of California, Merced, CA, USA.

[3]Institute for Atmospheric and Climate Science, ETH Zurich, Zurich, Switzerland.

[4]Aix Marseille Université, CNRS, IRD, INRA, Coll., CEREGE, Aix-en-Provence, France

Corresponding author: Michal Ben-Israel (mben-israel@ucmerced.edu)

†List of group authors for ASTER (Accélérateur pour les Sciences de la Terre) Team includes: R. Braucher, D.L. Bourlès, M. Arnold, G. Aumaître, K. Keddadouche

Key Points:

- We constructed a numerical model simulating sediment transport dynamics in large-scale fluvial systems constrained by cosmogenic nuclides.
- Examining data from four large rivers across the world, we constrain sediment residence time in large rivers.
- Estimated residence times of sediments in four large rivers across the world range 10^4-10^5 yr.

This article has been accepted for publication and undergone full peer review but has not been through the copyediting, typesetting, pagination and proofreading process, which may lead to differences between this version and the Version of Record. Please cite this article as doi: 10.1029/2021JF006417.

Abstract

The weathering of continental surfaces and the transport of sediments via rivers into the oceans is an integral part of the dynamic processes that shape the Earth's surface. To understand how tectonic and climatic forcings control regional rates of weathering, we must be able to identify their effects on sedimentary archives over geologic timescales. Cosmogenic nuclides are a valuable tool to study rates of surface processes and have long been applied in fluvial systems to quantify basin-wide erosion rates. However, in large rivers, continual processes of erosion and deposition during sediment transport make it difficult to constrain how long sediments spend within the fluvial system. In this study, we examine the role of rivers in buffering erosional signals by constraining the timescales of fluvial transport in large rivers across the world. We apply a stochastic numerical model based on measurements of cosmogenic nuclides concentrations and calculate sediment residence times of 10^4-10^5 years in large rivers. These timescales are equal to or longer than climatic cycles, implying that changes to rates of erosion brought on by climatic variations are buffered during transport in large rivers and may not be recognizable in the sedimentary record.

Plain Language Summary

Large rivers are the most effective agent for transporting sediment from the weathering continents into the oceans, with the world's biggest rivers draining nearly half of the continental surface. In this work, we calculate the time sediment spends in large rivers between weathering and deposition in four large rivers across the world. We do this by simulating the processes of sediment erosion and deposition in rivers and applying this model to new and existing data. The results of this model show that the time it takes for sand to be eroded from the source rock and transported down the river is tens to hundreds of thousands of years. These extended timescales mean that sediment transport in large rivers buffers the effect of climatic fluctuations on weathering rates. This finding can explain how seemingly contradictory evidence of climatic variations impact erosion rates, while products of erosion measured at the oceans show no significant changes during these times.

1 Introduction

The dynamic processes that shape the surface of our planet are governed by climate and tectonics, with temperature and precipitation dictating rates of weathering and rock uplift controlling erosion rates (e.g., DiBiase & Whipple, 2011; Perron, 2017). However, the influence of climate variability on denudation rates and erosion over geological timescales has been the subject of an ongoing debate. On one side, weathering rates in mountainous source regions show acceleration with variations in climatic conditions (e.g., Carretier et al., 2013; Ferrier et al., 2013; Tofelde et al., 2017). Conversely, records from sedimentary basins indicate that rates of sediment input into the oceans have remained stable throughout the late-Cenozoic (von Blanckenburg et al., 2015; Willenbring & von Blanckenburg, 2010). In this work, we examine sediment transport of the sand-sized fraction in four large rivers worldwide. We apply a stochastic numerical model that quantifies sediment residence times within fluvial systems based on sediment transport dynamics and constrained by measured and published cosmogenic nuclide data. These calculated residence times are key in understanding how transport through sedimentary systems can affect how changes

to rates of erosion at the source preserved in the sedimentary record (Castelltort & Van Den Driessche, 2003).

Transport of sediment in rivers is crucial for relating variations in long-term continental weathering rates to sedimentary archives that record climatic and tectonic events and the dynamic processes shaping the Earth's surface over geologic timescales (Armitage et al., 2011; Romans et al., 2016). Rivers are the most effective transport systems on the Earth's surface, with the world's largest rivers (with annual sediment discharge greater than ~15 megatons) draining nearly 50% of the Earth's continental surface (Milliman & Meade, 1983). To understand how the weathering signal is transferred from continental denudation to sedimentary basins, we need to consider the route that sediment takes within the fluvial transport system.

An idealized fluvial system can be divided into three parts (Schumm, 1977); the uppermost is the 'production zone', where slopes are steep, and weathering and erosion rates are high (Roering et al., 1999). Sediment is then transported downstream through the 'transport zone', an uninterrupted conduit for sediment, and is finally deposited in the sedimentary sink, the 'deposition zone' (Fig. 1). This simplified scheme is not applicable for large natural rivers, where deposition occurs intermittently during transport at the lower relief section of the 'transport zone'. In large-scale fluvial systems (with basins larger than ~$5 \cdot 10^5$ km^2), the transport zone is characterized by meandering and braiding streams, where processes such as channel bank erosion and accretion, and fluvial avulsion cause sediment to be temporarily stored in channel-bars and floodplains during transport downstream (Fig. 1; Hajek & Wolinsky, 2012; Mason & Mohrig, 2019). Continuous cycles of deposition and remobilization that occur stochastically within the transport zone have an important role in modulating sediment flux out of river systems. Depending on the nature and frequency of perturbations, fluvial processes have been shown to delay, buffer, and shred the weathering signal as it propagates through the fluvial system (Jerolmack & Paola, 2010; Romans et al., 2016). Constraining the timescales of sediment transport in large rivers allows a better understanding of which past environmental conditions can be reconstructed from the stratigraphic record and how (Meade, 1994; Sadler, 1981).

However, quantifying the timescales of fluvial transport in large rivers is not straightforward since the residence times of sediment, i.e., the timespan between weathering from the source until sediment accumulates in the sedimentary basin, is protracted by complex fluvial dynamics of intermittent deposition and temporary burial in the transport zone (Dunne et al., 1998; Lauer & Parker, 2008; Pizzuto, 1987). The many fluvial processes acting concurrently (i.e., sediment deposition and erosion at fluvial bars, floodplains, and riverbeds) make it extensively challenging to compute these processes reliably using a physical-based model alone (Straub et al., 2020). Geochemical dating methods, such as radiocarbon ages of terrestrial organic carbon, support the premise that inland riverine systems are more than passive pipes. Dating organic matter from rivers shows that fluvial transport processes influence the storage of organic matter in surface deposits leading to timescales reaching up to millennia. These timespans indicate that sediment is transported through a series of short transport events and long pauses (e.g., Clark et al., 2013;

Martin et al., 2013; Torres et al., 2017, 2020). Similarly, the timescales of weathering and transport of fine-grained clastic sediment (<63 μm) measured using U-series isotopes, range from 10^3 to 10^4 yr with large variability between the sampled large rivers (Dosseto et al., 2008; Granet et al., 2010; Vigier et al., 2001). Similar storage intervals for very fine sediment were also evaluated using meteoric ^{10}Be in the alluvial lowland rivers, the lower Amazon basin, and Rio Bermejo in Argentina (Repasch et al., 2020; Wittmann et al., 2018).

Although numerous previous studies were conducted to constrain sediment transport rates and evaluate their effects on natural processes, quantifying the residence time in large river systems remains a challenging task (Tofelde et al., 2021). Applying different geochemical proxies and dating methods to quantify residence times is similarly challenging due to the stochastic transport and continuous mixing of sediments (Carretier et al., 2020). Previous works examining changes in cosmogenic nuclide concentrations from sampling locations along the large rivers have demonstrated how an increase in exposure time does not necessarily correlate with distance downstream (Wittmann et al., 2020). Here we present a stochastic numerical model simulating fluvial transport dynamics of sediment erosion and deposition. We constrain the sediment transport times using the exposure times at different depths calculated based on two independently produced cosmogenic nuclides (^{10}Be and ^{26}Al) measured in quartz sands from four large rivers across the world. This approach allows us to combine a process-based model with measured data yielding better constraints on the residence time of the sand-sized fraction in large rivers and enabling us to assess the implications of fluvial transport on the buffering of continental erosion signals and the preservation of changes to environmental conditions in sedimentary archives.

2 Materials and Methods

2.1 Modeling approach

Previous means to evaluate sediment transport in rivers have included mathematical solutions for sediment diffusion in fluvial basins and mass balance calculations of sediment storage and transport (e.g., Carretier et al., 2020; Castelltort & Van Den Driessche, 2003; Li et al., 2018; Paola et al., 1992; Pizzuto, 1987, 2020; Straub et al., 2020). These different approaches reflect the diverse fluvial processes that operate over a range of timescales.

To overcome complexities arising from the various individual processes leading to sediment storage in large rivers, we constrain timescales of fluvial transport of silicate sand in large rivers using a probabilistic numerical model that computes sediment residence times based on measurements of cosmogenic ^{26}Al and ^{10}Be in modern fluvial sand. To do so, we use a simplified time-evolving model that accounts for the concentration of cosmogenic ^{10}Be and ^{26}Al in the sediment at each time-step, where production is dependent on time and burial depth (due to attenuation of cosmic ray particles through the sediment) and loss is dependent on time and radioactive decay constants. A decrease in burial depth can represent erosion from the top or dispersal and re-deposition, resulting in higher cosmogenic nuclide production rates. Similarly, an increase in burial depth can represent deposition on top or re-deposition at a new deeper depth

(and slower production rates). Hence, sediment thickness at each time-step represents the different sedimentary processes, including continuous sediment mixing and erosion, transport, and re-deposition. This approach allows for a multitude of erosional processes varying temporally, regardless of spatial scale.

The presented model does not directly consider sediment fluxes or the geography of the fluvial system, but rather applies a synthetic burial and travel history for each bundle of grains of sand. The specific synthetic history of each bundle produces a time series of ^{10}Be and ^{26}Al concentrations. By producing different histories at random, the model allows for a wide spectrum of scenarios, which can be compared to measured concentrations from multiple sampling sites along a downstream transect of a river. Each of the acceptable model simulations is considered as a "successful run". These narrow down the spectrum of acceptable scenarios for a specific sample and provide an estimate for the family of scenarios realized in the sample as well as the acceptable range of transport times for the sample.

Only a handful of publications present measurements of more than one cosmogenic nuclide from several locations along the flow path of large rivers. We examine cosmogenic ^{10}Be and ^{26}Al concentrations measured in sand-sized (125-850 μm) quartz samples from transects along the lower basin of the Colorado River (this work, see Supporting Information), the Amazon lowlands (Wittmann, von Blanckenburg, Maurice, Guyot, Filizola, et al., 2011), the Branco River, a tributary of the Amazon (Wittmann, von Blanckenburg, Maurice, Guyot, & Kubik, 2011), and the Po River (Wittmann et al., 2016). Examining the concentrations of two independent cosmogenic nuclides makes for a strong constrain on the simulated concentrations produced by the model, and using data from multiple sampling sites along a downstream transect enables us to account for natural variability, ultimately leading to a better and more realistic examination of cosmogenic nuclide production during transport in large rivers.

2.2 Applying cosmogenic ^{10}Be and ^{26}Al to quantify residence time

Terrestrial in-situ cosmogenic nuclides, produced within minerals at or near the surface by secondary cosmic-ray interactions, are widely applied to study surface processes by dating the exposure of surfaces and sediments, quantifying basin-wide erosion rates, and evaluating burial and deposition times (Dunai, 2010; Gosse & Phillips, 2001). Here, we examine changes to ^{10}Be and ^{26}Al concentrations measured in quartz grains produced during transport in large rivers. Generally, the total measured cosmogenic nuclide concentration in any quartz grain is the result of accumulation during bedrock erosion and downslope transport (the inherited component), and the nuclides produced during alluvial transport at varying rates depending on burial depth and duration during intermittent storage (the transport component). The inherited component depends on the rate of erosion, which can also change with time.

To account for production during erosion at the source, we assume that the ratio of ^{26}Al to ^{10}Be is consistent with production at the surface (^{26}Al/^{10}Be = 6.75 in quartz, Balco et al., 2008). This assumption is reasonable even when considering the effect of slow rates of bedrock erosion on the initial ^{26}Al/^{10}Be ratio. In all of the source regions of the presented rivers, bedrock erosion rates are

not slow and are estimated to range between 40-1350 mm/kyr (Champagnac et al., 2007; Matmon et al., 2012; Safran et al., 2005).

The other component contributing to the concentration of cosmogenic nuclides produced in situ in the river sediment is the 'transport component', produced over multiple cycles of deposition and erosion during fluvial transport and storage within the fluvial system. To account for this component, we determined the concentration of each of the measured radioactive nuclides (N) for each model time-step (i) by the production and decay rates, which can be expressed by (Dunai, 2010; Lal, 1991):

$$(1)\ N_i = N_{i-1}e^{-\lambda t_i} + \frac{P_{total}}{\lambda}\left(1 - e^{-\lambda t_i}\right),$$

where N_{i-1} is the inherited concentration of the cosmogenic nuclide from the previous step, λ is the decay constant in yr^{-1} (with half-lives of 0.708±0.017 and 1.387±0.012 Myr for ^{26}Al and ^{10}Be, respectively, Chmeleff et al., 2010; Korschinek et al., 2010), P_{total} is the production rate for both spalleogenic and muonic production at a subsurface depth z, and t is the time interval for which the sediment was buried at a depth z. For both nuclides, spalleogenic and muonic production decreases exponentially with depth (z) and can be described by:

$$(2)\ P(z_i) = P_{sp}e^{\frac{-\rho z_i}{\Lambda_{sp}}} + P_{mu}e^{\frac{-\rho z_i}{\Lambda_{mu}}},$$

where ρ is the density of the sediment (2200 $kg \cdot m^{-3}$ for quartz sand) and Λ is the attenuation length in $kg \cdot m^{-2}$ ($1.6 \cdot 10^3$ for neutron spallation [sp] and $1.5 \cdot 10^4$ for muons [mu], Balco, 2017). Production (P) is calculated for the mean latitude and elevation in the sampling region based on the scheme presented by Stone (2000; Table 1). Due to the extensive nature of these fluvial systems, they cover several degrees of latitude and longitude. However, when examining possible changes in the Amazon, Po, and Colorado rivers, these variations are negligible (<10%) in the total production rate calculations.

2.3 Stochastic simulations

2.3.1 Initial ^{10}Be concentration

The cosmogenic nuclide concentration of each of the analyzed samples is composed of cosmogenic nuclides produced during erosion at the source and during transport in the fluvial system. For that reason, we assume that the lowest measured concentration along a river represents erosion at the source plus the least amount of ^{10}Be produced during transport. While it is likely that some of the measured ^{10}Be concentration was produced during transport, this conservative estimation accounts for varying (slower) rates of erosion at the source as well as exposure prior to temporary deposition in the sampling location. For each of the presented rivers (Table 1), the initial ^{10}Be concentration (N_0) is drawn from a uniform random distribution with values running between zero and the maximum equal to the lowest concentration of ^{10}Be (including uncertainty) measured in the analyzed samples. The significance of this assumption to the model results is that calculated residence times are *minimum* times. While the overall residence time of sediment in the fluvial system increases downstream, this does not necessarily entail an increase in cosmogenic exposure

time between downstream sampling locations. This behavior can be observed in the nonlinear changes of cosmogenic ^{10}Be and ^{26}Al concentrations downstream presented in this work (see Table S1 in the Supporting Information) and the referenced material (Wittmann et al., 2011; Wittmann et al., 2016), and is likely due to the complexity of sediment transport dynamics in the low relief section of the transport zone and continuous mixing. Because we cannot assume that sediment exposure time simply increases downstream, we use the highest measured value of ^{10}Be in each river independent of its relative distance from the source. We assume steady-state erosion rates at the source and calculate ^{26}Al concentration based on the production ratio of ^{26}Al/^{10}Be at the surface in quartz (~6.75).

2.3.2 Synthetic sedimentary history

Burial time intervals are generated randomly using an exponential distribution so that recently deposited sediment is more likely to be eroded (Lauer & Parker, 2008; Lauer & Willenbring, 2010; Malmon et al., 2003). Model simulations continued until either the simulation is successful, namely, the cosmogenic nuclides concentration for the synthetic history fits the observed concentrations, or it was unsuccessful for at least 10^6 years, meaning that this synthetic history is not acceptable. Burial depths are randomly chosen from a uniform distribution around the mean burial depth that represents the depth where the number of successful runs was highest for each river (see figures S3-S6 in the Supporting Information). These distribution types were chosen to better represent the cycle of deposition, burial, and erosion (Lauer & Parker, 2008; Lauer & Willenbring, 2010; Malmon et al., 2003; Pizzuto et al., 2017). In their model, Torres et al. (2017) tested the different possible distributions and found that a Pareto distribution better describes the burial time intervals for their results. However, these tests also show that an exponential distribution describes the results well and is the next best choice. Here we choose to use a simple exponential distribution as this type of distribution is well suited for the type of model constructed here because it only depends on one parameter (μ) and allows for calibration when using small sample sets.

As most previous works evaluate sediment transport times of 10^4-10^6 years (Blöthe & Korup, 2013; Carretier et al., 2020; Fülöp et al., 2020; Repasch et al., 2020), we run the model for a maximal time of 10^6 years and a maximum of 10^6 time-steps. The maximal time dictates a time after which if the simulated results do not match the measured results, the model run is considered unsuccessful. At each model time-step, we calculate the concentrations of ^{26}Al and ^{10}Be based on nuclide-specific production at the determined burial depth and radioactive decay. Production rates are normalized to the averaged elevation and latitude for each river (Table 1).

The modeled concentrations of ^{10}Be and ^{26}Al were calculated iteratively for each sampling site at each of the four examined rivers. The simulation stopped when the modeled concentrations of both nuclides were simultaneously equal to the measured concentrations within natural analytical uncertainty (see an example from the Colorado River in the Supporting Information; fig S1). If the measured value was reached, the simulation was considered "successful". For each successful run, we saved the minimal and maximal modeled times when an agreement was reached

(corresponding to minimal and maximal cosmogenic measurements uncertainties). The residence time for each successful run is defined as the median between the two end-results with the range as its uncertainty (see an example from the Amazon River in the Supporting Information; fig S2).

2.4 Sensitivity analyses and model calibration

The sensitivity of the model results to the number of simulations was tested based on one example (in the range of 1 to $10 \cdot 10^5$ simulations). The result showed that 1000 simulations were enough to reach a value within the measurement uncertainty (Fig. 2). Therefore, the model was run 1000 times for each of the samples. In each of the 1000 runs, the calculation can be considered as if it is a single grain of sand. Each of these grains has its own stochastic history with random burial depths and time intervals spent at each depth. Therefore, when examining the simulation results at a specific site, we take a thousand different "grains", each with its own separate history. The result is obtained from the distribution of the grains within each site.

The model was calibrated separately for each river for the parameters of the depth range of 0-50 m and timespan of 0-5000 years. The model parameters for each river were determined based on the burial and time intervals that produced the highest number of successful runs considering all the samples at each river (see figs. S3-S6 in the Supporting Information). This way, while success rates can be lower for a specific sample at a river, the model parameters presumably represent the fluvial process at this particular river. Since the parameters of the random distributions are unknown, the model was calibrated so that its success rate (the ratio of successful to total runs) was maximized for all the samples together within each river, thus resulting in more universal parameters. Furthermore, since each simulation produced a different residence time, calibration using the success rate promised that the results were as reliable as in such a stochastic framework.

3 Results

Residence times for each of the sampling locations at each of the four rivers is calculated from the successful simulations out of 1000 runs of the model and presented as boxplots (Fig. 3). Within the four studied rivers, the model has successfully simulated the measured cosmogenic nuclide concentrations for 16 out of 20 examined sampling locations with the lowest success rates of 47% calculated at the Branco River for sampling location Br8b2 (Table 1). The highest success rate was 100%, for 11 out of a total of 20 samples from all rivers (three out of six in the Amazon River, one out of five in the Branco River, all three samples in the Po River, and four out of six in the Colorado River; Table 1). At the Amazon River, four out of the five sampling sites examined reached the measured ^{10}Be and ^{26}Al concentrations within analytical uncertainty, except for site Ir0.4c. While both Ir0.4c and Ir0.4b were sampled at the confluence with Rio Iriri, 0.4 km from the left bank (Wittmann et al., 2011), sample Ir0.4c shows higher measured ^{10}Be and ^{26}Al concentrations compared to the rest of the Amazon samples. Similarly, at the Branco River, four out of the five sampling locations showed similar measured concentrations except for Br5b sampled at the exact location as Br5c but separated for a different grain-size fraction (250-500 µm and 500-800 µm, accordingly). All three sites at the Po River and only four out of the six sites at the Lower Colorado River reached the measured ^{10}Be and ^{26}Al concentrations.

Cases where the model has failed to simulate the measured ^{10}Be and ^{26}Al concentrations (0% success rate), can be the result of different physical conditions at the sampling site that are not represented by the model parameters chosen for the river (mean burial depth and time). Alternatively, low success rates can be the result of sediments at the sampling sites not being part of the dynamic transport processes (i.e., abandoned terraces or locations that are controlled by localized erosional processes). Both of these scenarios are part of the natural variability within large-scale fluvial systems. The success rate at each river, calculated as a simple mean of the simulations for all samples including unsuccessful samples, is ≥65%, with the highest success rates at the Po River and the lowest at the Branco River (Table 1). Including the unsuccessful runs in the reported success rate, allows us to include the synthetic histories for all the sediments sampled in each of the rivers and demonstrates that the modeling approach presented here is viable and can be used to calculate sediment residence time in the examined rivers.

For most of the examined rivers, success rates, as well as residence times, show high sensitivity to mean burial depths and low sensitivity to mean burial times <500 years, except for the Po River which only shows sensitivity to mean burial times (see figs. S3-S6 in the Supplementary Information). Therefore, the mean minimum burial depth was determined per river and ranges between a minimum of two meters in the Branco River and a maximum of 20 m in the Amazon River, while the mean burial time chosen is 20 years for all rivers. Mean burial depth also appears to correlate with the flux of suspended sediments in the rivers (Kettner & Syvitski, 2008; Meade, 1994; Milliman & Meade, 1983). Our model shows little sensitivity to timescales shorter than 500 years, as these are fast compared to cosmogenic nuclide production rates. An average of 20 years for burial time-steps is short compared to burial times measured and estimated for sedimentary units in fluvial systems (e.g., Torres et al., 2017; Jerolmack and Mohrig, 2007; Repasch et al., 2020). However, the average time-step presented here represents smaller-scale fluvial processes reflected by changes in burial depth of a single grain of sand and therefore are expected to be shorter compared to burial time of a sedimentary unit.

The residence times of the successful runs at each of the examined rivers are presented as box plot distributions with a residence time median for each sampling site (Fig. 3). Within each of the four studied rivers, residence times mostly agree between the different sampling locations, except for site Par0.9a at the Amazon River that shows shorter residence times ranging between 0 years (i.e., faster than ~1000 years given the uncertainty range of cosmogenic nuclide concentrations) and ~650 kyr and a median of ~300 kyr. However, residence times vary significantly between the different rivers with the longest median residence times medians calculated at the Amazon River ranging ~300-600 kyr and the shortest median residence times at the Po River ranging from ~20 to 35 kyr. The Branco and Colorado rivers show similar ranges of median residence times of ~200-250 kyr at the Branco River, and 200-400 kyr at the Colorado River, except for site PD which shows a median residence time of ~800 kyr. The median residence times at the different rivers appear to agree with the basin size and length of the rivers. Even though the model is not spatially constrained, this trend agrees with the basic concept of the model, as longer rivers would allow for more events of intermittent burial that would result in longer residence times overall.

Overall, for all rivers, the high degree of freedom of the model, the relatively small range of residence times for each river together with high model success rates (≥65%), versus the large deviation of residence times among the different rivers, strengthen the validity of the model results. Additionally, the calculated ranges agree with previous evaluations of inorganic sediment storage from Himalayan Rivers (Blöthe & Korup, 2013) and, to some degree, with lag-times from the

Murray-Darling basin in Australia (Fülöp et al., 2020). These results lead us to ascertain that overall residence times of 10^4-10^5 yr reached by our model are indeed a reliable quantification.

4 Discussion

4.1 Model viability

A recent analysis of cosmogenic nuclides from over 50 large rivers shows that in 65% of the examined rivers, $^{26}Al/^{10}Be$ ratios are within the uncertainty of the surface-production-rate ratio. In contrast, for the other 35%, ratios were significantly lower (Wittmann et al., 2020). However, attempting to resolve sediment residence times in the fluvial system cannot be achieved using $^{26}Al/^{10}Be$ ratios since these analyses are not sensitive enough to record the periodic and prolonged burial of sediment at shallow depths that occurs frequently within the low relief section of the transport zone. Thus, sediment residence times in large rivers cannot be directly evaluated using measured concentrations based on a single cosmogenic nuclide nor the calculated $^{26}Al/^{10}Be$ burial ages separately. Both the concentrations and their ratio must be considered simultaneously. Because nuclide production rates at or near the surface are much faster than decay rates, the overall ^{26}Al and ^{10}Be concentrations increase with residence time during shallow burial, while their $^{26}Al/^{10}Be$ ratio will show little change.

Our model differs from previous applications of cosmogenic nuclides in fluvial systems as it simulates sediment transport and storage in the low relief section of the transport zone of large rivers by accounting for stochastic intermittent erosion and deposition at shallow depths and brief time intervals. The model results show that even small variations in the $^{26}Al/^{10}Be$ ratio may represent long residence times of sediments within rivers at shallow burial depths (see an example from the Amazon River in Fig. S2 in the Supporting Information). Using two separate cosmogenic nuclides with different production rates and decay rates, the model can account for production with varying sediment cover and sedimentary processes, resulting in longer timescales that are more representative than simple exposure age calculations. Constraining model simulations of sediment transport dynamics with measured concentrations of cosmogenic nuclides produces a realistic determination of residence times of silicate sand in large rivers.

A potential source for variations in the cosmogenic nuclide production rates that should be considered are changes to the intensity and orientation of the Earth's geomagnetic field over 10^3-10^4 yr timescales (Pigati & Lifton, 2004). These changes may affect the calculated residence time in the model. For three out of the four studied fluvial systems, timescales of sediment transport are one to two orders of magnitude longer, so these variations are averaged during transport. This is not the case for the Po River, where transport is at the 10^4 yr timescale (Table 1). Yet, considering the geographical location of the Po River, changes in production rates of ^{10}Be resulting from changes in the geomagnetic field over time are smaller than 5% (Pigati & Lifton, 2004).

We, therefore, propose that the presented model provides an accurate and more realistic "age" for the sediment than the more common exposure or burial age applications of cosmogenic nuclides. We use this calculated "age" to quantify the residence time of sand-sized quartz sediment transported by large rivers.

4.2 Geologic implications

The timescales of sediment transport in large rivers dictate how upstream perturbations to continental weathering are communicated downstream. To distinguish signal perturbations at the outlet of a river, the intrinsic response time of the river, recorded in sediment residence times, must be significantly shorter compared to the perturbations themselves. Otherwise, transport in the fluvial systems will buffer the signal by the time it reaches the outlet of the river (Straub et al., 2020). Therefore, we must consider the timescales of fluvial transport compared to environmental forcings that control weathering rates. Climatic cycles, such as glacial-interglacial periods, Milankovitch cycles, and other shorter climatic oscillations, trigger large changes in temperature and precipitation that affect weathering rates (Lupker et al., 2013). However, these variations operate over timescales ranging from decades to tens of thousands of years (Abe-Ouchi et al., 2013; Fig. 5). The timescales of fluvial transport calculated here are 10^4-10^5 yr, within the same range or longer compared to climatic variations.

Prolonged sediment residence times, together with complex sedimentary dynamics in large rivers (Gärtner et al., 2020), lead to downstream signal attenuation. The implication of which is the dampening of the signal of climatic cycles (as well as uncommon short-term, $<10^5$ yr, tectonic events) on rates of weathering recorded in sedimentary archives. Conversely, as tectonic forcings primarily operate over timescales that are longer by at least an order of magnitude compared to rates of fluvial transport (Nance & Murphy, 2013), the difference in timescales implies that variations to weathering rates brought on by tectonic events will mostly be preserved in the sedimentary record.

5 Conclusions

The intrinsic response time of rivers manifested as sediment residence times cannot be measured directly and has been primarily calculated from a mass balance (sediment budget) perspective. We simulate sediment transport dynamics and produce reliable residence times for sand-sized sediment in large rivers using a stochastic model, constrained with cosmogenic nuclide data sampled from the low-relief section of the transport zone of four large rivers worldwide. This approach enables us to examine how continuous intermitted burial and erosion cycles during transport in large-scale fluvial systems lead to prolonged residence times of 10^4-10^5 years.

Changes in sedimentation rates observed in large river deltas and sedimentary archives are considered to represent changes in denudation rates (Allen, 2008). Previous works have linked changes in sediment deposition to climatic forcing, concluding that these are the result of acceleration in continental erosion rates (e.g., Clift & Giosan, 2014; Goodbred Jr & Kuehl, 2000; Peizhen et al., 2001). However, with contradicting evidence for the impact of climate on erosion rates (e.g., von Blanckenburg et al., 2015; Willenbring & von Blanckenburg, 2010), the question of whether and to what extent do sediments deposited in the deep ocean represent erosion in the source regions remains open (Molnar, 2004; Schumer & Jerolmack, 2009). The residence times presented in this work agree with previous evaluations that have been shown to buffer the

perturbations in the continental erosion signal with timescales $<10^5$ yr (Castelltort & Van Den Driessche, 2003; e.g., Romans et al., 2016; Straub et al., 2020). This observation denotes that variations to erosion rates caused by climatic cycles will be buffered by fluvial transport, concluding that climate-induced changes in denudation rates at the source will most likely be buffered during transport will not be preserved in sedimentary archives (e.g., Carretier et al., 2013; Ferrier et al., 2013; Tofelde et al., 2017).

The outcomes of the presented research, further illustrate the importance of rivers for deciphering how the different forces that impact landscape evolution are recorded in sedimentary archives and call for further examination on how climate-induced erosional signals can be implicitly deduced from sedimentary archives.

Acknowledgments

This research was supported by the Israel Science Foundation Individual Research Grant no. 385/14 to AM. This work was also partially supported by the BSF Prof. Rahamimoff Travel Grant for Young Scientists to MBI. MA was supported by an ETH Zurich Postdoctoral Fellowship (project no. 21-1 FEL-67), by the Stiftung für naturwissenschaftliche und technische Forschung and the ETH Zürich Foundation. We would also like to thank Aaron Sims and Yonaton Goldschmidt for their assistance in the field and Yona Geller and Ofir Tirosh for their help with sample preparation. Lastly, we appreciate all the hard work and constructive comments by Laure Guerit, Hugh Sinclair, Marisa Repasch, and anonymous reviewers. The authors declare no known conflict of interests.

Open Research

Cosmogenic nuclide data analyzed in this study are available in the referenced published literature for the Po River (Wittmann et al., 2016) and Amazon and Branco rivers (Wittmann et al., 2011). Cosmogenic nuclide data for the lower Colorado River are available in SI Table S1.
All the codes used in this study have been described in published work and are available in the public domain. The sediment residence time model was accomplished using the MATLAB® software and is available in the Supporting Information. All codes needed to run the model are available on https://github.com/michalbenisrael/SedRes.

References

Abe-Ouchi, A., Saito, F., Kawamura, K., Raymo, M. E., Okuno, J., Takahashi, K., & Blatter, H. (2013). Insolation-driven 100,000-year glacial cycles and hysteresis of ice-sheet volume. *Nature*, *500*(7461), 190–193. https://doi.org/10.1038/nature12374

Allen, P. A. (2008). From landscapes into geological history. *Nature*, *451*(7176), 274–276. https://doi.org/10.1038/nature06586

Armitage, J. J., Duller, R. A., Whittaker, A. C., & Allen, P. A. (2011). Transformation of tectonic and climatic signals from source to sedimentary archive. *Nature Geoscience*, *4*(4), 231–235. https://doi.org/10.1038/ngeo1087

Balco, G., Stone, J. O., Lifton, N. A., & Dunai, T. J. (2008). A complete and easily accessible means of calculating surface exposure ages or erosion rates from 10Be and 26Al measurements. *Quaternary Geochronology*, *3*(3), 174–195. https://doi.org/10.1016/j.quageo.2007.12.001

von Blanckenburg, F., Bouchez, J., Ibarra, D. E., & Maher, K. (2015). Stable runoff and weathering fluxes into the oceans over Quaternary climate cycles. *Nature Geoscience*, *8*(7), 538–542. https://doi.org/10.1038/ngeo2452

Blöthe, J. H., & Korup, O. (2013). Millennial lag times in the Himalayan sediment routing system. *Earth and Planetary Science Letters*, *382*, 38–46. https://doi.org/10.1016/j.epsl.2013.08.044

Carretier, S., Regard, V., Vassallo, R., Aguilar, G., Martinod, J., Riquelme, R., et al. (2013). Slope and climate variability control of erosion in the Andes of central Chile. *Geology*, *41*(2), 195–198. https://doi.org/10.1130/G33735.1

Carretier, S., Guerit, L., Harries, R., Regard, V., Maffre, P., & Bonnet, S. (2020). The distribution of sediment residence times at the foot of mountains and its implications for proxies recorded in sedimentary basins. *Earth and Planetary Science Letters*, *546*, 116448. https://doi.org/10.1016/j.epsl.2020.116448

Castelltort, S., & Van Den Driessche, J. (2003). How plausible are high-frequency sediment

supply-driven cycles in the stratigraphic record? *Sedimentary Geology*, *157*(1–2), 3–13. https://doi.org/10.1016/S0037-0738(03)00066-6

Champagnac, J. D., Molnar, P., Anderson, R. S., Sue, C., & Delacou, B. (2007). Quaternary erosion-induced isostatic rebound in the western Alps. *Geology*, *35*(3), 195. https://doi.org/10.1130/G23053A.1

Chmeleff, J., von Blanckenburg, F., Kossert, K., & Jakob, D. (2010). Determination of the 10Be half-life by multicollector ICP-MS and liquid scintillation counting. *Nuclear Instruments and Methods in Physics Research Section B: Beam Interactions with Materials and Atoms*, *268*(2), 192–199. https://doi.org/10.1016/j.nimb.2009.09.012

Clark, K. E., Hilton, R. G., West, A. J., Malhi, Y., Gröcke, D. R., Bryant, C. L., et al. (2013). New views on "old" carbon in the Amazon River: Insight from the source of organic carbon eroded from the Peruvian Andes. *Geochemistry, Geophysics, Geosystems*, *14*(5), 1644–1659. https://doi.org/10.1002/ggge.20122

Clift, P. D., & Giosan, L. (2014). Sediment fluxes and buffering in the post- glacial Indus Basin. *Basin Research*, *26*(3), 369–386.

DiBiase, R. A., & Whipple, K. X. (2011). The influence of erosion thresholds and runoff variability on the relationships among topography, climate, and erosion rate. *Journal of Geophysical Research*, *116*(F4), F04036. https://doi.org/10.1029/2011JF002095

Dosseto, A., Bourdon, B., & Turner, S. P. (2008). Uranium-series isotopes in river materials: Insights into the timescales of erosion and sediment transport. *Earth and Planetary Science Letters*, *265*(1–2), 1–17. https://doi.org/10.1016/j.epsl.2007.10.023

Dunai, T. J. (2010). *Cosmogenic Nuclides: Principles, Concepts and Applications in the Earth Surface Sciences*. (Intergovernmental Panel on Climate Change, Ed.). Cambridge:

Cambridge University Press.

Dunne, T., Mertes, L. A. K., Meade, R. H., Richey, J. E., & Forsberg, B. R. (1998). Exchanges of sediment between the flood plain and channel of the Amazon River in Brazil. *Bulletin of the Geological Society of America*, *110*(4), 450–467. https://doi.org/10.1130/0016-7606(1998)110<0450:EOSBTF>2.3.CO;2

Ferrier, K. L., Huppert, K. L., & Perron, J. T. (2013). Climatic control of bedrock river incision. *Nature*, *496*(7444), 206–209. https://doi.org/10.1038/nature11982

Foreman, B. Z., & Straub, K. M. (2017). Autogenic geomorphic processes determine the resolution and fidelity of terrestrial paleoclimate records. *Science Advances*, *3*(9), e1700683.

Fülöp, R. H., Codilean, A. T., Wilcken, K. M., Cohen, T. J., Fink, D., Smith, A. M., et al. (2020). Million-year lag times in a post-orogenic sediment conveyor. *Science Advances*, *6*(25), eaaz8845. https://doi.org/10.1126/sciadv.aaz8845

Gärtner, A., Merchel, S., Niedermann, S., Braucher, R., Steier, P., Rugel, G., et al. (2020). Nature Does the Averaging—In-Situ Produced 10Be, 21Ne, and 26Al in a Very Young River Terrace. *Geosciences*, *10*(6), 237. https://doi.org/10.3390/geosciences10060237

Goodbred Jr, S. L., & Kuehl, S. A. (2000). Enormous Ganges-Brahmaputra sediment discharge during strengthened early Holocene monsoon. *Geology*, *28*(12), 1083–1086.

Gosse, J. C., & Phillips, F. M. (2001). Terrestrial in situ cosmogenic nuclides:theory and application. *Quaternary Science Reviews*, *20*, 1475–1560. https://doi.org/10.1016/S0277-3791(00)00171-2

Granet, M., Chabaux, F., Stille, P., Dosseto, A., France-Lanord, C., & Blaes, E. (2010). U-series disequilibria in suspended river sediments and implication for sediment transfer time in

alluvial plains: The case of the Himalayan rivers. *Geochimica et Cosmochimica Acta*, *74*(10), 2851–2865. https://doi.org/10.1016/j.gca.2010.02.016

Hajek, E. A., & Wolinsky, M. A. (2012). Simplified process modeling of river avulsion and alluvial architecture: Connecting models and field data. *Sedimentary Geology*, *257–260*, 1–30. https://doi.org/10.1016/j.sedgeo.2011.09.005

Jerolmack, D. J., & Paola, C. (2010). Shredding of environmental signals by sediment transport. *Geophysical Research Letters*, *37*(19).

Kettner, A. J., & Syvitski, J. P. M. (2008). Predicting discharge and sediment flux of the Po River, Italy since the Last Glacial Maximum. In *Analogue and Numerical Modelling of Sedimentary Systems: From Understanding to Prediction*. Wiley-Blackwell Oxford, UK.

Korschinek, G., Bergmaier, A., Faestermann, T., Gerstmann, U. C., Knie, K., Rugel, G., et al. (2010). A new value for the half-life of 10Be by Heavy-Ion Elastic Recoil Detection and liquid scintillation counting. *Nuclear Instruments and Methods in Physics Research Section B: Beam Interactions with Materials and Atoms*, *268*(2), 187–191. https://doi.org/10.1016/j.nimb.2009.09.020

Lal, D. (1991). Cosmic ray labeling of erosion surfaces: in situ nuclide production rates and erosion models. *Earth and Planetary Science Letters*, *104*(2–4), 424–439. https://doi.org/10.1016/0012-821X(91)90220-C

Lauer, J. W., & Parker, G. (2008). Modeling framework for sediment deposition, storage, and evacuation in the floodplain of a meandering river: Theory. *Water Resources Research*, *44*(4), W04425. https://doi.org/10.1029/2006WR005528

Lauer, J. W., & Willenbring, J. (2010). Steady state reach-scale theory for radioactive tracer concentration in a simple channel/floodplain system. *Journal of Geophysical Research*,

115(F4), F04018. https://doi.org/10.1029/2009JF001480

Li, Q., Gasparini, N. M., & Straub, K. M. (2018). Some signals are not the same as they appear: How do erosional landscapes transform tectonic history into sediment flux records? *Geology*, *46*(5), 407–410. https://doi.org/10.1130/G40026.1

Lupker, M., France-Lanord, C., Galy, V., Lavé, J., & Kudrass, H. (2013). Increasing chemical weathering in the Himalayan system since the Last Glacial Maximum. *Earth and Planetary Science Letters*, *365*, 243–252. https://doi.org/10.1016/j.epsl.2013.01.038

Malmon, D. V., Dunne, T., & Reneau, S. L. (2003). Stochastic Theory of Particle Trajectories through Alluvial Valley Floors. *The Journal of Geology*, *111*(5), 525–542. https://doi.org/10.1086/376764

Martin, E. E., Ingalls, A. E., Richey, J. E., Keil, R. G., Santos, G. M., Truxal, L. T., et al. (2013). Age of riverine carbon suggests rapid export of terrestrial primary production in tropics. *Geophysical Research Letters*, *40*(21), 5687–5691. https://doi.org/10.1002/2013GL057450

Mason, J., & Mohrig, D. (2019). Differential bank migration and the maintenance of channel width in meandering river bends. *Geology*, *47*(12), 1136–1140. https://doi.org/10.1130/G46651.1

Matmon, A., Stock, G. M., Granger, D. E., & Howard, K. A. (2012). Dating of Pliocene Colorado River sediments: Implications for cosmogenic burial dating and the evolution of the lower Colorado River. *Geological Society of America Bulletin*, *124*(3–4), 626–640. https://doi.org/10.1130/B30453.1

Meade, R. H. (1994). Suspended sediments of the modern Amazon and Orinoco rivers. *Quaternary International*, *21*, 29–39. https://doi.org/10.1016/1040-6182(94)90019-1

Milliman, J. D., & Meade, R. H. (1983). World-Wide Delivery of River Sediment to the Oceans.

The Journal of Geology, *91*(1), 1–21. https://doi.org/10.1086/628741

Molnar, P. (2004). Late Cenozoic Increase in Accumulation Rates of Terrestrial Sediment: How Might Climate Change Have Affected Erosion Rates? *Annual Review of Earth and Planetary Sciences*, *32*(1), 67–89. https://doi.org/10.1146/annurev.earth.32.091003.143456

Nance, R. D., & Murphy, J. B. (2013). Origins of the supercontinent cycle. *Geoscience Frontiers*, *4*(4), 439–448.

Paola, C., Heller, P. L., & Angevine, C. L. (1992). The large-scale dynamics of grain-size variation in alluvial basins, 1: Theory. *Basin Research*, *4*(2), 73–90. https://doi.org/10.1111/j.1365-2117.1992.tb00145.x

Peizhen, Z., Molnar, P., & Downs, W. R. (2001). Increased sedimentation rates and grain sizes 2–4 Myr ago due to the influence of climate change on erosion rates. *Nature*, *410*(6831), 891–897.

Perron, J. T. (2017). Climate and the Pace of Erosional Landscape Evolution. *Annual Review of Earth and Planetary Sciences*, *45*(1), 561–591. https://doi.org/10.1146/annurev-earth-060614-105405

Pigati, J. S., & Lifton, N. A. (2004). Geomagnetic effects on time-integrated cosmogenic nuclide production with emphasis on in situ 14C and 10Be. *Earth and Planetary Science Letters*, *226*(1–2), 193–205. https://doi.org/10.1016/j.epsl.2004.07.031

Pizzuto, J. (1987). Sediment diffusion during overbank flows. *Sedimentology*, *34*(2), 301–317.

Pizzuto, J. (2020). Suspended sediment and contaminant routing with alluvial storage: New theory and applications. *Geomorphology*, *352*, 106983.

Pizzuto, J., Keeler, J., Skalak, K., & Karwan, D. (2017). Storage filters upland suspended sediment signals delivered from watersheds. *Geology*, *45*(2), 151–154.

Repasch, M., Wittmann, H., Scheingross, J. S., Sachse, D., Szupiany, R., Orfeo, O., et al. (2020). Sediment Transit Time and Floodplain Storage Dynamics in Alluvial Rivers Revealed by Meteoric 10Be. *Journal of Geophysical Research: Earth Surface*, *125*(7). https://doi.org/10.1029/2019JF005419

Roering, J. J., Kirchner, J. W., & Dietrich, W. E. (1999). Evidence for nonlinear, diffusive sediment transport on hillslopes and implications for landscape morphology. *Water Resources Research*, *35*(3), 853–870.

Romans, B. W., Castelltort, S., Covault, J. A., Fildani, A., & Walsh, J. P. (2016). Environmental signal propagation in sedimentary systems across timescales. *Earth-Science Reviews*, *153*, 7–29. https://doi.org/10.1016/j.earscirev.2015.07.012

Sadler, P. M. (1981). Sediment accumulation rates and the completeness of stratigraphic sections. *The Journal of Geology*, *89*(5), 569–584.

Safran, E. B., Bierman, P. R., Aalto, R., Dunne, T., Whipple, K. X., & Caffee, M. (2005). Erosion rates driven by channel network incision in the Bolivian Andes. *Earth Surface Processes and Landforms*, *30*(8), 1007–1024. https://doi.org/10.1002/esp.1259

Schumer, R., & Jerolmack, D. J. (2009). Real and apparent changes in sediment deposition rates through time. *Journal of Geophysical Research*, *114*, F00A06. https://doi.org/10.1029/2009JF001266

Schumm, S. A. (1977). *The Fluvial System*. New: John Wiley and Sons.

Stone, J. O. (2000). Air pressure and cosmogenic isotope production. *Journal of Geophysical Research: Solid Earth*, *105*(B10), 23753–23759. https://doi.org/10.1029/2000JB900181

Straub, K. M., Duller, R. A., Foreman, B. Z., & Hajek, E. A. (2020). Buffered, Incomplete, and Shredded: The Challenges of Reading an Imperfect Stratigraphic Record. *Journal of*

Geophysical Research: Earth Surface, *125*(3). https://doi.org/10.1029/2019JF005079

Tofelde, S., Schildgen, T. F., Savi, S., Pingel, H., Wickert, A. D., Bookhagen, B., et al. (2017). 100 kyr fluvial cut-and-fill terrace cycles since the Middle Pleistocene in the southern Central Andes, NW Argentina. *Earth and Planetary Science Letters*, *473*, 141–153.

Tofelde, S., Bernhardt, A., Guerit, L., & Romans, B. W. (2021). Times Associated With Source-to-Sink Propagation of Environmental Signals During Landscape Transience. *Frontiers in Earth Science*, *9*. https://doi.org/10.3389/feart.2021.628315

Torres, M. A., Limaye, A. B., Ganti, V., Lamb, M. P., West, A. J., & Fischer, W. W. (2017). Model predictions of long-lived storage of organic carbon in river deposits. *Earth Surface Dynamics*, *5*(4), 711–730. https://doi.org/10.5194/esurf-5-711-2017

Torres, M. A., Kemeny, P. C., Lamb, M. P., Cole, T. L., & Fischer, W. W. (2020). Long-term storage and age- biased export of fluvial organic carbon: field evidence from West Iceland. *Geochemistry, Geophysics, Geosystems*.

Vigier, N., Bourdon, B., Turner, S., & Allègre, C. J. (2001). Erosion timescales derived from U-decay series measurements in rivers. *Earth and Planetary Science Letters*, *193*(3–4), 549–563. https://doi.org/10.1016/S0012-821X(01)00510-6

Willenbring, J. K., & von Blanckenburg, F. (2010). Long-term stability of global erosion rates and weathering during late-Cenozoic cooling. *Nature*, *465*, 211–214. Retrieved from https://doi.org/10.1038/nature09044

Wittmann, H., von Blanckenburg, F., Maurice, L., Guyot, J. L., & Kubik, P. W. (2011). Recycling of Amazon floodplain sediment quantified by cosmogenic 26Al and 10Be. *Geology*, *39*(5), 467–470. https://doi.org/10.1130/G31829.1

Wittmann, H., von Blanckenburg, F., Maurice, L., Guyot, J. L., Filizola, N., & Kubik, P. W.

(2011). Sediment production and delivery in the Amazon River basin quantified by in situ-produced cosmogenic nuclides and recent river loads. *Geological Society of America Bulletin*, *123*(5–6), 934–950. https://doi.org/10.1130/B30317.1

Wittmann, H., Malusà, M. G., Resentini, A., Garzanti, E., & Niedermann, S. (2016). The cosmogenic record of mountain erosion transmitted across a foreland basin: Source-to-sink analysis of in situ 10 Be, 26 Al and 21 Ne in sediment of the Po river catchment. *Earth and Planetary Science Letters*, *452*, 258–271. https://doi.org/10.1016/j.epsl.2016.07.017

Wittmann, H., Oelze, M., Roig, H., & von Blanckenburg, F. (2018). Are seasonal variations in river-floodplain sediment exchange in the lower Amazon River basin resolvable through meteoric cosmogenic 10Be to stable 9Be ratios? *Geomorphology*, *322*, 148–158. https://doi.org/10.1016/j.geomorph.2018.08.045

Wittmann, H., Oelze, M., Gaillardet, J., Garzanti, E., & von Blanckenburg, F. (2020). A global rate of denudation from cosmogenic nuclides in the Earth's largest rivers. *Earth-Science Reviews*, *204*, 1–17. https://doi.org/10.1016/j.earscirev.2020.103147

Figure and Table Captions

Figure 1. Schematic diagram of sediment transport in large-scale fluvial systems. Sediment is mainly produced in the mountainous region upstream (the Production Zone) and is transported to the depositional basin (Deposition Zone). As sediments reach the downstream low-relief section of the transport zone, they are intermittently deposited at floodplains and channel bars for varying periods and depths represented here by shades of brown. Storage in a specific point in space occurs until an erosional process remobilizes and transports the sediment further downstream. These continuous cycles of erosion and deposition lead to a complex storage framework of sediment within the fluvial system and make it difficult to quantify the transport time of sediments in rivers. The graph on the bottom left shows changes in sediment flux as a function of time (after Straub et al., 2020). The perturbation in sediment flux due to climate-induced increase in erosion rates at the

production zone (red) is buffered when the signal reaches the deposition zone (blue) because of the residence times of sediment in the low-relief section of the transport zone.

Figure 2. Sensitivity of the model to the number of runs. Probability of the maximal calculated residence time from 1-10^5 model runs for sample CRWB (Colorado River) with burial depth 10 m and burial time 100 years. The spread of residence time of 1000 runs (purple) is smaller than the natural analytical uncertainty calculated from cosmogenic nuclide concentrations (see Table S1 in the Supporting Information), allowing for a reliable calculation of residence times. This test was applied for all rivers and produced similar results.

Figure 3. Boxplots of calculated residence times from the four examined rivers. Each box presents all calculated residence times for 1000 runs, with a maximum of 10^6 steps and a maximal run time of 10^6 yr (see specific river parameters in Table 1). The central red mark is the median, and the bottom and top blue edges of the box indicate 25th and 75th percentiles, respectively. The dashed whiskers extend to the most extreme data points, which are not considered outliers (the presented dataset does not contain outliers).

Figure 4. The residence time of sand-sized silicate sediments in large rivers. (**A**) Box plot of calculated residence times and percentage of successful runs for each sample in the Branco River. (**B**) Map of the corresponding sampling stations along the Branco River. (**C**) Map showing the locations of the rivers analyzed in this work and the model results. Sediment residence time is presented as the range of medians (RM) calculated for each sample in a specific river. n - number of samples analyzed, and SI is the averaged success rate from all stations.

Figure 5. A comparison of timescales of fluvial transport and major tectonic and climatic variations. Timescales of fluvial transport represent sediment residence times in large rivers reported here as well as published lag times and sediment storage from large rivers across the globe (Blöthe & Korup, 2013; Clift & Giosan, 2014; Fülöp et al., 2020). Climatic cycles are after Foreman and Straub (2017). ENSO stands for El Niño–Southern Oscillation, and NAO stands for North Atlantic Oscillation. Tectonic cycles are after Meade (1994). The timescales of fluvial transport are longer or similar to climatic variations and mostly shorter compared to tectonic variations, implying that climatic variations and short-term tectonic events will be buffered by the fluvial transport system and will not be preserved in the sedimentary record.

Table 1. Model Variables and Data

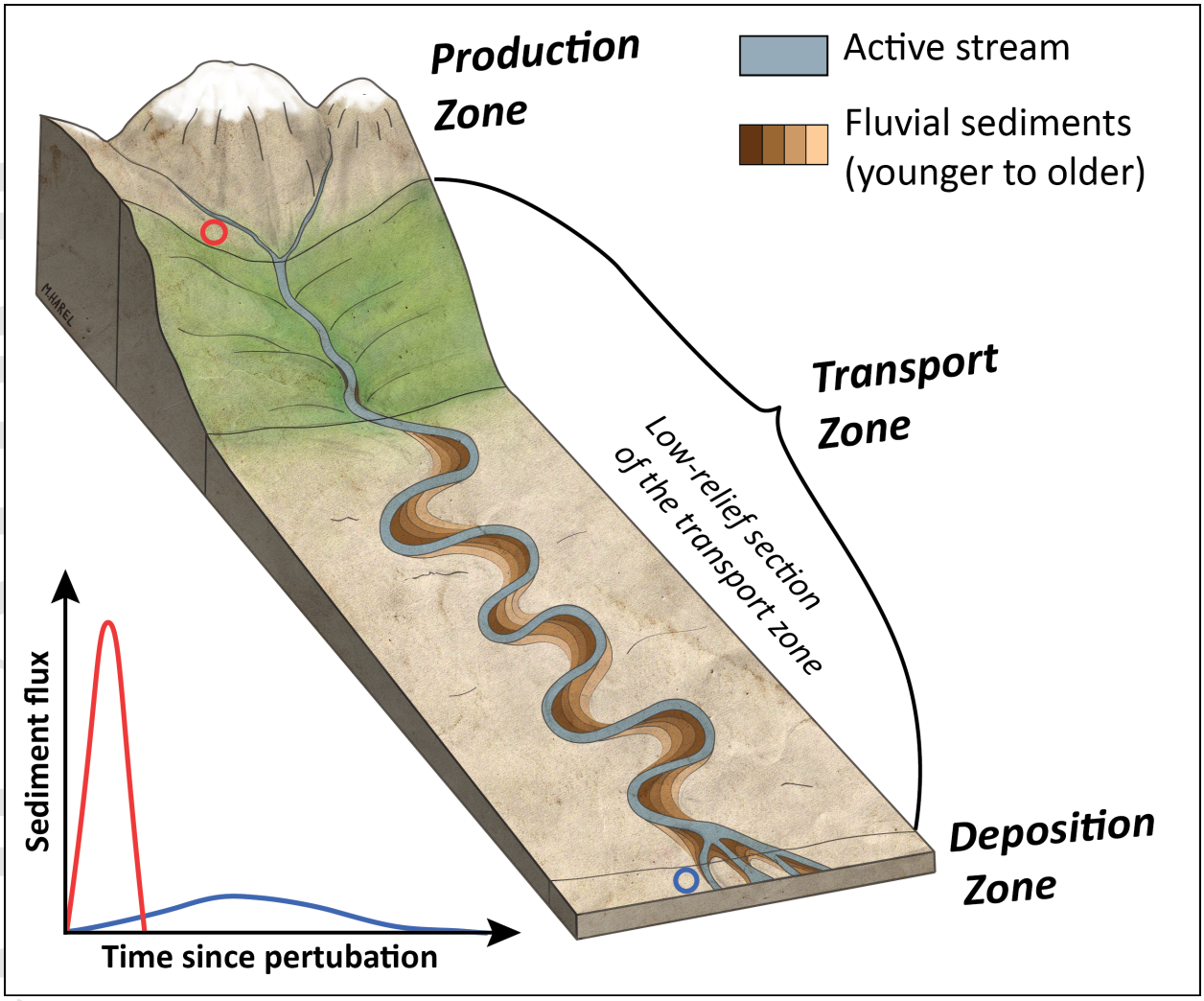

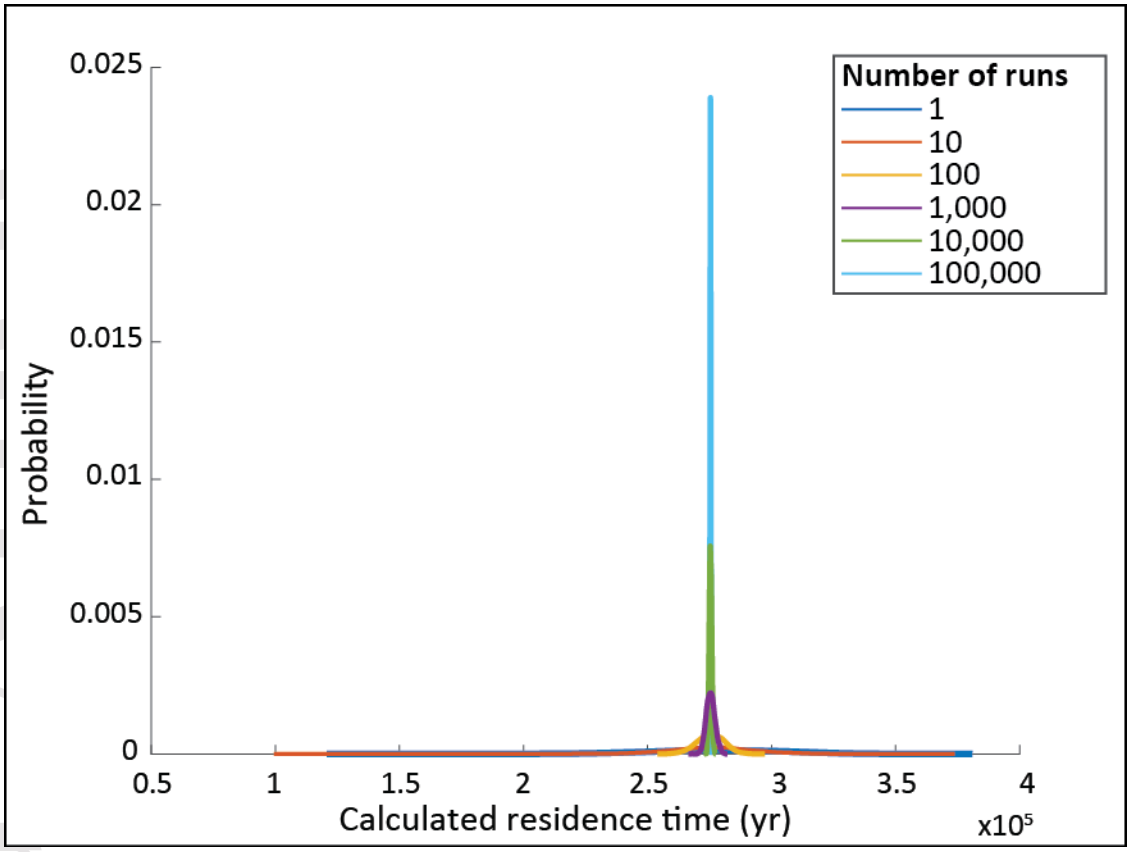

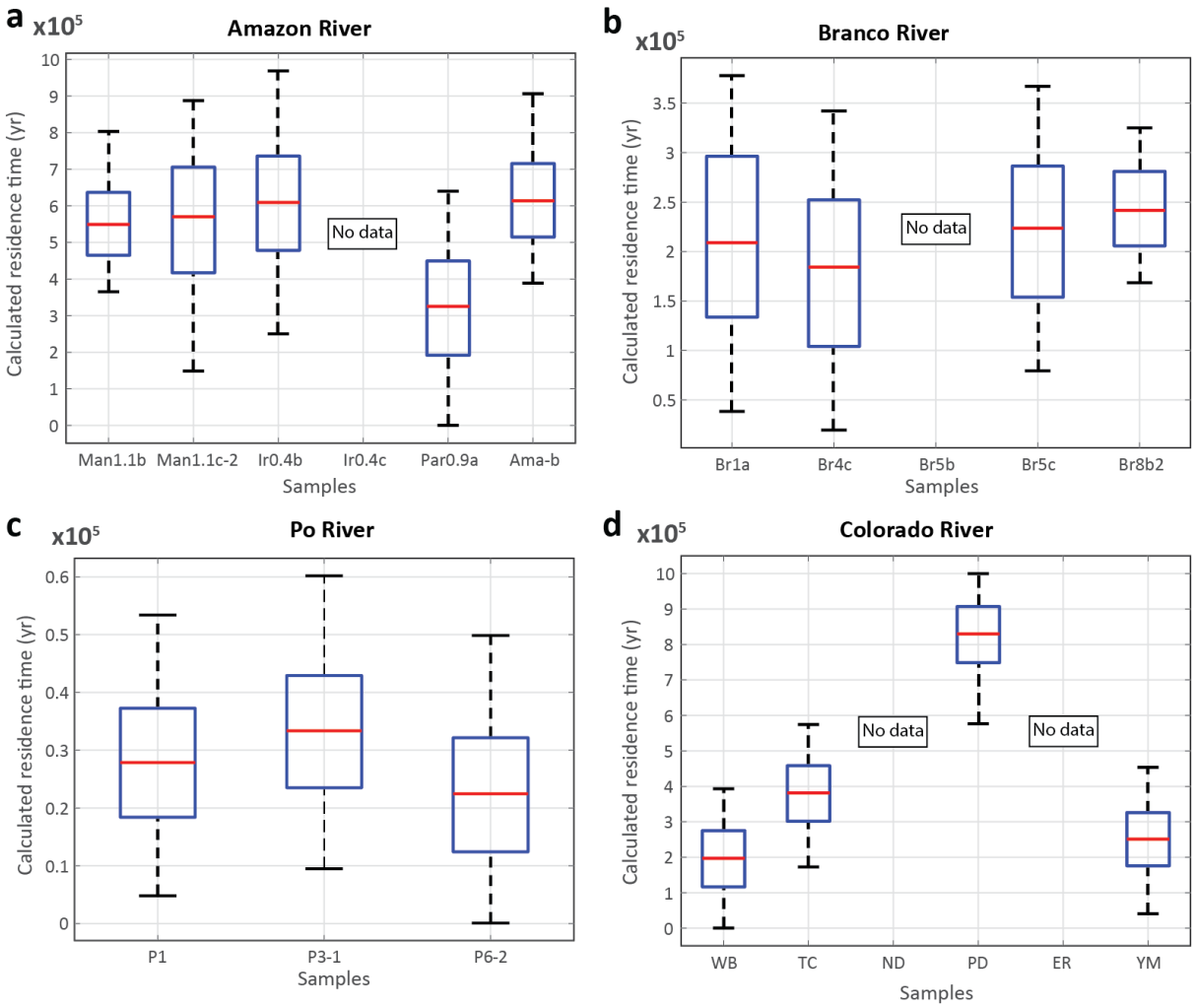

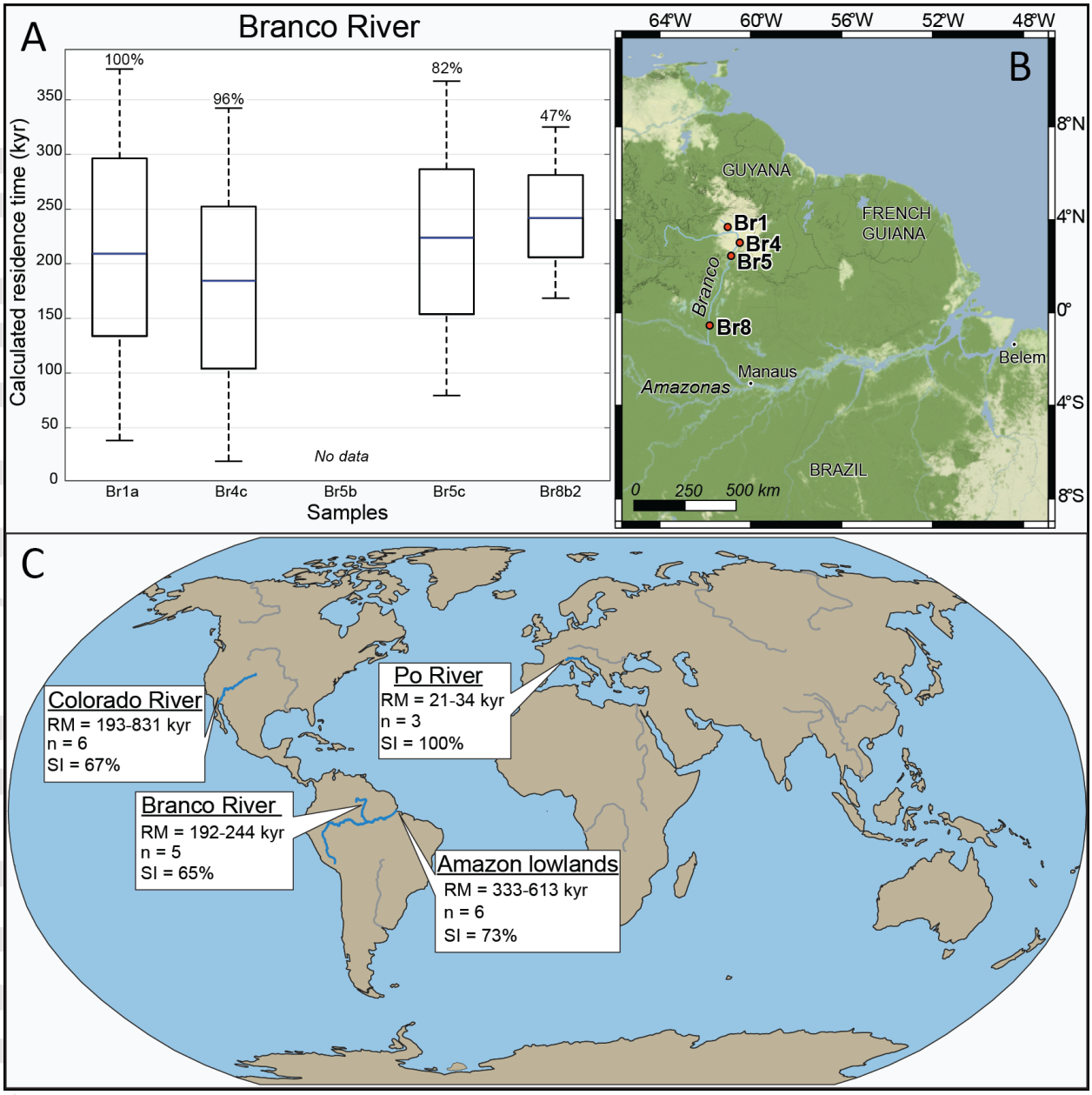

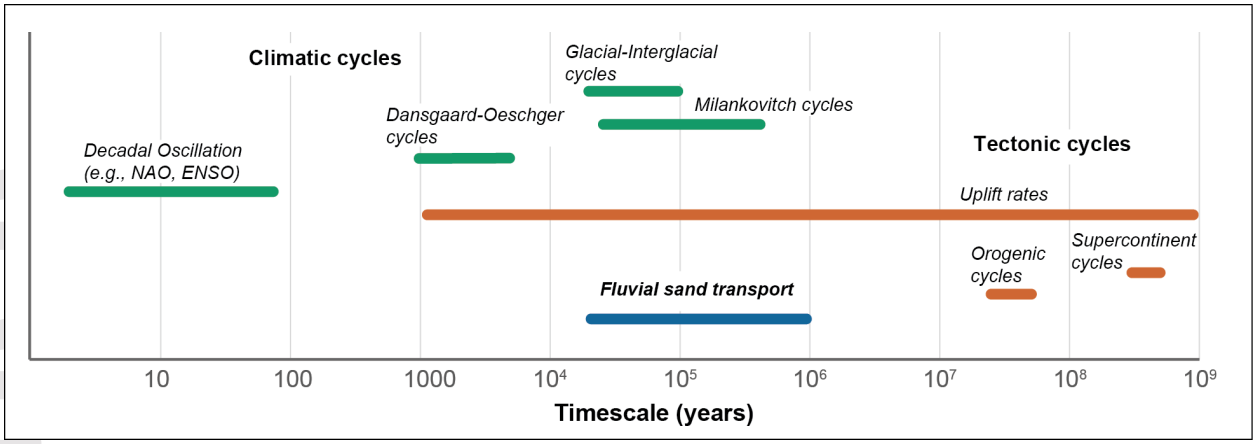

Table 1. Model Variables and Data

River	No. of samples	Samples names	Latitude[a] (°N)	Elevation[b] (m a.s.l)	Averaged Scaled Production Rate[c] ^{26}Al (atoms g^{-1} yr^{-1})	Averaged Scaled Production Rate[c] ^{10}Be (atoms g^{-1} yr^{-1})	Mean Burial Depth[d] (m)	Mean Burial Time[e] (year)	Successful Runs[f] (%)	Median Residence Time[f] (10^3 yr)
Amazon[g]	6	Man 1.1b, Man 1.1c2, Ir0.4b, Ir0.4c, Par0.9a, Ama-b	1	5	17.84	2.92	20	20	72.9 (62.6, 100, 100, 0, 100, 74.5)	561.4 (551.8 , 561.4 , 333.3 , 612.7 , 612.5)
Branco[h]	5	Br1a, Br4c, Br5b, Br5c, Br8b2	1	50	18.47	3.03	2	20	64.9 (100, 95.9, 0, 82.1, 46.5)	214.4 (216.1 , 192.3 , 212.7 , 244.2)
Po[i]	3	P1, P3-1, P6-2	45	50	32.32	5.30	6	20	100 (100, 100, 100)	28.7 (28.7, 33.8, 21.0)
Colorado[j]	6	CRWB, CRTC, CRND, CRPD, CRER, CRYM	33	100	27.29	4.47	10	20	67 (100, 100, 0, 0, 100, 100)	314.2 (193.3 , 380.5 , 831.0 , 247.8)

Comments:

[a] Mean latitude in sampling region

[b] Mean elevation in sampling region

[c] Scaled using the scheme presented by Stone (2000)

[d] Mean of random distribution determined based on best model results, see sensitivity tests figures in the Supporting Information.

[e] Mean of exponential distribution determined based on best model results, see sensitivity tests figures in the Supporting Information .

[f] Mean of modeled samples (result per sample)

[g] Wittmann et al. (2011a)

[h] Wittmann et al. (2011b)

[i] Wittmann et al. (2016).

[j] This work (see Supporting Information)